

## Recent Development of Large-Scale Shell-Model and Projected Shell Model

H.-K. Wang<sup>1</sup>, Y. Sun<sup>2</sup>, F.-Q. Chen<sup>3</sup>, Y.-Q. He<sup>4</sup>, S.-F. Li<sup>1</sup>

<sup>1</sup>College of Physics and Telecommunication Engineering,

Zhoukou Normal University, Henan 466000, People's Republic of China

<sup>2</sup>Department of Physics and Astronomy, Shanghai Jiao Tong University,  
Shanghai 200240, People's Republic of China

<sup>3</sup>Departamento de Fisica Teorica, Universidad Autdnoma de Madrid,  
E-28049 Madrid, Spain

<sup>4</sup>College of mathematics and statistics, Zhoukou Normal University,  
Henan 466000, People's Republic of China

Received 23 November 2015

**Abstract.** To describe excitations around a deformation equilibrium, especially for those nuclei without a well-defined shape, we have developed two kinds of shell models: large-scale shell model based on a spherical basis and projected shell model based on a deformed basis. As examples, we show level spectra of a near-spherical nucleus  $^{130}\text{In}$  calculated by the large-scale shell-model. The Hamiltonian adopts pairing-plus-multipole force with monopole corrections, and the model space is sufficiently large that includes six proton orbits and seven neutron orbits to allow both proton and neutron core-excitations. In another development to treat shape effects in heavy, deformed nuclei, improved shell-model wave functions are introduced to the projected shell model by superimposing angular-momentum and particle-number projected states constructed with different quadrupole-deformation and pairing-gap parameters as two-dimensional generator coordinates. Using these as trial wave functions, we solve the Hill-Wheeler Equation and analyze the obtained results for the transitional Gd isotopes.

PACS codes: 21.60.Cs, 21.10.Re, 21.60.Ev

### 1 Introduction

Nuclei are among the few quantum systems where one can discuss them in terms of shape [1]. Different shapes of nuclei correspond to fundamentally different nuclear wave functions that characterize the microscopic motions of nucleons. A large number of nuclei in the nuclear chart can be understood with well-defined shapes, either spherical or deformed. However, there are known cases where

more interesting situations can occur, as for instance, coexistence of different shapes within one nucleus [2].

Theoretical methods have been developed to treat nuclei belonging to different shapes. These correspond to different truncation schemes. For example, for nuclei near the closed shells, one usually needs to handle a few particle- or hole-orbits near the closed shells and allows many possible excitations among them. For example, the relatively simple structure of the near doubly-closed-shell nucleus,  $^{132}\text{Sn}$ , is recognized in their observed spectra which are usually understood as consisting of two types of excitations: excitations of valence single particles and excited states formed by couplings of the valence nucleons to core excitations. There have been successful calculations for the nuclei around  $^{132}\text{Sn}$  by the shell-model groups, which may be divided into two classes, treating, separately, the two types of excitations. The low-energy states were studied by using the shell-model method with the effective interaction derived from the CD-Bonn potential. On the other hand, the high-energy (and often high-spin) states of core excitations were simply interpreted with empirical nucleon-nucleon interactions. These two classes of calculations work for their own applicable states. However, to study the interplay between them and understand the structure problem as a whole, it is desired to have a unified treatment for the two types of excited states in a manageable shell-model calculation.

For nuclei in the rare-earth region around neutron number  $N = 90$ , it is well known that the isotopes there undergo a shape transition from near-spherical to well-deformed systems, and description of the transitional region needs special consideration. The transitional nuclei do not have a definite shape and a microscopical description would require a superposition of many Slater determinants. In this paper, we briefly discuss the recent shell-model developments in the above two directions by taking respective examples.

## 2 Large-Scale Shell Model Based on Spherical Basis

Recently, we have proposed a shell-model Hamiltonian [3, 4] for the particle- and hole-nuclei around  $^{132}\text{Sn}$ . The large-scale shell model, called the EPQQM model [5–8], employs a set of separable forces as the effective interaction, including the  $J = 0$  and  $J = 2$  pairing terms, the quadrupole-quadrupole term, the octupole-octupole term, and the monopole corrections

$$H = H_{sp} + H_{P_0} + H_{P_2} + H_{QQ} + H_{OO} + H_{mc}. \quad (1)$$

While the  $P_0$ ,  $P_2$ ,  $QQ$ , and  $OO$  terms, with the properly chosen strengths, take care of the global property of spectrum, correct single-particle energies  $H_{sp}$  and the monopole corrections  $H_{mc}$  are responsible for changes in the shell evolution. It turns out that this simple Hamiltonian with only a few parameters can be applied to describe not only the low-energy levels but also those of high energies characterized by core-excitations for the  $^{132}\text{Sn}$  region [3, 4, 9, 10].

Recent Development of Large-Scale Shell-Model and Projected Shell Model

In the work reported in Ref. [4], the level spectra with the structure were discussed by the hole-orbit couplings and core excitations for some  $Z < 50$  nuclei close to  $^{132}\text{Sn}$ . The model space consisted of six proton orbits ( $0f_{5/2}, 1p_{3/2}, 1p_{1/2}, 0g_{9/2}, 0g_{7/2}, 1d_{5/2}$ ) and seven neutron ones ( $0g_{7/2}, 1d_{5/2}, 2s_{1/2}, 0h_{11/2}, 1d_{3/2}, 1f_{7/2}, 2p_{3/2}$ ), in which the proton orbits ( $0g_{7/2}, 1d_{5/2}$ ) above the  $Z = 50$  shell for proton core-excitations and the neutron ones ( $1f_{7/2}, 2p_{3/2}$ ) above the  $N = 82$  shell for neutron core-excitations were included. The shell-model code NUSHELLX [12] was used for the calculation.

Relative to the double-magic  $^{132}\text{Sn}$ ,  $^{130}\text{In}$  is an odd-odd nucleus with one proton-hole and one neutron-hole. The shape of its ground state is almost spherical. Therefore, the low-lying levels of  $^{130}\text{In}$  is formed by couplings of the proton and neutron single-hole configurations. The shell-model results of  $^{130}\text{In}$  is shown in Figure 1. The configuration of  $\pi g_{9/2}^{-1} \nu h_{11/2}^{-1}$  is predicted as

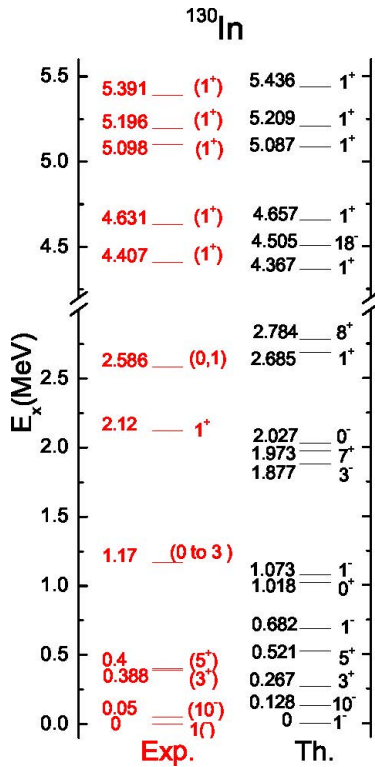


Figure 1. (Color online) This example shows the results from the large-scale shell-model calculation using the EPQQM interaction for  $^{130}\text{In}$  and comparison with experimental data [11]. The figure is taken from Figure 5 of Ref. [4].

the dominant component for the ground state, which consists of ten members from  $I^\pi = 1^-$  to  $10^-$ . The level of  $1^-$  is the ground state, and  $10^-$  at 128 keV corresponds to the experimental level  $10^-$  at 50 keV. As shown in Figure 1, the  $1^+$  level at 2.685 MeV has a hole-configuration of  $\pi g_{9/2}^{-1} \nu g_{7/2}^{-1}$ . The other  $1^+$  levels above this level, up to 5.5 MeV in excitation, are all core-excited states in our shell-model predictions. Without the extended shell-model space we could not be able to calculate these states. A comparison of these  $1^+$  levels with data and their proposed core-excited configurations are given in Table 1.

Table 1. The predicted  $1^+$  levels in  $^{130}\text{In}$  with their main configurations. Available experimental data are displayed for comparison.

	Exp.	Th.	Conf.
1+	2.12	2.685	$\pi g_{9/2}^{-1} \nu g_{7/2}^{-1}$
(1+)	4.407	4.367	$\pi p_{1/2}^{-1} \nu h_{11/2}^{-2} f_{7/2}$
(1+)	4.63	4.657	$\pi p_{1/2}^{-1} \nu h_{11/2}^{-2} f_{7/2}$
(1+)	5.098	5.087	$\pi p_{1/2}^{-1} \nu h_{11/2}^{-2} f_{7/2}$
(1+)	5.196	5.209	$\pi g_{9/2}^{-1} \nu d_{3/2}^{-1} h_{11/2}^{-1} f_{7/2}$
(1+)	5.391	5.436	$\pi g_{9/2}^{-1} \nu d_{3/2}^{-1} h_{11/2}^{-1} f_{7/2}$

### 3 Projected Shell Model Based on Deformed Basis

The Projected Shell Model (PSM) [13] has been successful in the microscopic description of the yrast properties of rotational nuclei and high-spin bands with multi-quasiparticle (qp) structures. In those studies one usually starts with a fixed deformation of the mean-field (with either axial or triaxial symmetry), and the dynamics is obtained through mixing various qp configurations preserving the symmetries. However, for description of soft nuclei of the transitional region, the original PSM has not been successful. Next, we report on another recent development [14] by superimposing different intrinsic states corresponding to different deformations. We diagonalize the shell model Hamiltonian by solving the Hill-Wheeler equation [15] in the basis spanned by the angular-momentum- and particle-number-projected states.

As in the original PSM [13] one superimposes qp-states with good symmetries, now we take projected states associated with different axial deformation,  $\epsilon_2$ , and superimpose them:

$$|\Psi^{I,N}\rangle = \int d\epsilon_2 f^{I,N}(\epsilon_2) \hat{P}^I \hat{P}^N |\Phi_0(\epsilon_2)\rangle, \quad (2)$$

where  $\hat{P}^I$  and  $\hat{P}^N$  are the projection operators on good angular momentum and particle number, restoring the rotational symmetry violated in the de-

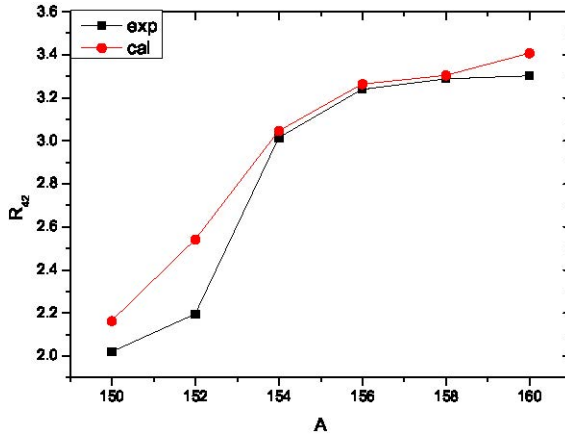


Figure 2. (Color online) Comparison of calculated energy ratio  $E(4_1^+)/E(2_1^+)$  for  $^{150-160}\text{Gd}$  with the experimental ones.

formed mean-field and the gauge symmetry violated in the BCS approximation.  $|\Phi_0(\epsilon_2)\rangle$  in (2) is a Nilsson+BCS state, i.e. the qp vacuum with deformation  $\epsilon_2$ . For each  $\epsilon_2$ , a set of Nilsson single-particle states can be generated, with the Nilsson parameter  $\kappa, \mu$  taken from Ref. [16]. The concept is originally from the Generator Coordinate Method (GCM) [15]. Detailed model structure can be found in Ref. [14].

To see what effects the new model can bring, we use the important indicator for the onset of deformation: the energy ratio  $R_{42} = E(4_1^+)/E(2_1^+)$ . It is well-known that for vibrational nuclei (spherical) one has  $R_{42} \sim 2.0$ . For well deformed nuclei with a rotational spectrum  $E(I) \propto I(I+1)$ , one has  $R_{42} \sim 3.33$ . At the critical point of shape phase transition, which may be described by the  $X(5)$  dynamical symmetry [17], one has  $R_{42} \sim 3.0$ . It is seen in Figure 2 that  $R_{42}$  is indeed close to 2.0 for  $^{150}\text{Gd}$  and to 3.33 for  $^{156-160}\text{Gd}$ . For  $^{154}\text{Gd}$ ,  $R_{42}$  is approximately 3.0, which suggests that along the isotopic chain, the location of the critical point lies at  $^{154}\text{Gd}$  with  $N = 90$ .

The improved PSM wave functions superimpose the symmetry-conserved states with different deformations. This is important particularly for nuclei lying in the transitional region where no definite shape can be associated with them. The effect of performing the GCM type of calculation for those ‘‘soft’’ nuclei can be clearly seen in Figure 3. In this figure, results from two calculations are presented. Black squares correspond to the full GCM calculation and red dots to the usual PSM calculation with assumption of a fixed deformation for each nucleus. It can be easily concluded from the figure that for well-deformed nuclei such as  $^{156,158,160}\text{Gd}$ , there are no much differences between the results of the two calculations, meaning that the original PSM [13] is already a good approximation

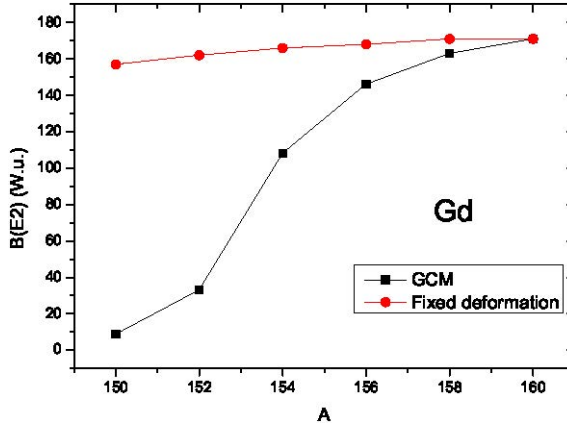


Figure 3. (Color online) Comparison of two calculations for  $B(E2)$  transitions from the first  $2^+$  state to the ground state for  $^{150-160}\text{Gd}$ : black squares corresponding to the full GCM calculation and red dots to the calculation with a fixed deformation.

to the general GCM treatment for well-deformed nuclei. However, qualitative differences are seen for the light isotopes. The much smaller  $B(E2)$  transitions for  $^{150,152,154}\text{Gd}$  can only be obtained by the full GCM treatment.

#### 4 Conclusions

We have briefly introduced two recent developments for shell models, namely, large-scale shell model based on spherical basis and projected shell model based on deformed basis. The same type of Hamiltonian including pairing-plus-multipole forces are employed in both calculations. Two corresponding examples have been shown. With the spherical shell model, the level spectrum analysis is carried out for hole-nuclei  $^{130}\text{In}$ . We emphasized that for the model space we include neutron and proton core excitations. We also discussed the new step made beyond the original Projected Shell Model to build many-body wave functions as a superposition of symmetry-conserved states with different quadrupole deformations  $\epsilon_2$ . We have shown, by taking the  $N = 86 - 96$  isotopes of  $^{150-160}\text{Gd}$  as examples, that with the same set of parameters, the observed transitional behavior is reasonably reproduced by our microscopic calculations. The characteristic features of qualitatively different systems before and after the shape phase transition can thus be clearly distinguished.

This work is in collaboration with K. Kaneko, M. Hasegawa, T. Mizusaki, S. Tazaki, and P. Ring. It is partially supported by the National Natural Science Foundation of China (Nos. 11505302, 11575112, 11135005) and by the 973 Program of China (No. 2013CB834401).

## References

- [1] A. Bohr and B.R. Mottelson (1975) *Nuclear Structure*, Vol. 2, Benjamin, New York.
- [2] K. Heyde and J.L. Wood (2011) *Rev. Mod. Phys.* **83** 1467.
- [3] H. Jin, M. Hasegawa, S. Tazaki, K. Kaneko, and Y. Sun (2011) *Phys. Rev. C* **84** 044324.
- [4] H.-K. Wang, Y. Sun, H. Jin, K. Kaneko, and S. Tazaki (2013) *Phys. Rev. C* **88** 054310.
- [5] M. Hasegawa, K. Kaneko, and S. Tazaki (2001) *Nucl. Phys. A* **688** 765.
- [6] K. Kaneko, M. Hasegawa, and T. Mizusaki (2002) *Phys. Rev. C* **66** 051306(R).
- [7] K. Kaneko, Y. Sun, M. Hasegawa, and T. Mizusaki (2008) *Phys. Rev. C* **78** 064312.
- [8] K. Kaneko, Y. Sun, M. Hasegawa, and T. Mizusaki (2011) *Phys. Rev. C* **83** 014320.
- [9] H.-K. Wang, K. Kaneko, Y. Sun (2014) *Phys. Rev. C* **89** 064311.
- [10] H.-K. Wang, K. Kaneko, Y. Sun (2015) *Phys. Rev. C* **91** 021303(R).
- [11] <http://www.nndc.bnl.gov/ensdf/>.
- [12] W. Rae, NUSHELLX code, <http://knollhouse.org>.
- [13] K. Hara and Y. Sun (1995) *Int. J. Mod. Phys. E* **4** 637.
- [14] F.-Q. Chen, Y. Sun, and P. Ring (2013) *Phys. Rev. C* **88** 014315.
- [15] D.J. Hill and J.A. Wheeler (1953) *Phys. Rev.* **89** 1102.
- [16] S.G. Nilsson (1955) *Mat. Fys. Medd. Dan. Vidensk. Selsk.* **29** no. 16.
- [17] F. Iachello (2001) *Phys. Rev. Lett.* **87** 052502.